

**High-fidelity synchronization and transfer of quantum states in optomechanical hybrid systems**Hugo Molinares <sup>\*</sup>*Centro de Óptica e Información Cuántica, Universidad Mayor, Camino la Piramide 5750, Huechuraba, Santiago, Chile*Vitalie Eremeev<sup>†</sup>*Instituto de Ciencias Básicas, Facultad de Ingeniería y Ciencias, Universidad Diego Portales, Avenida Ejército 441, Santiago, Chile*Miguel Orszag<sup>‡</sup>*Centro de Óptica e Información Cuántica, Universidad Mayor, camino la Piramide 5750, Huechuraba, Santiago, Chile and Instituto de Física, Pontificia Universidad Católica de Chile, Casilla 306, Santiago, Chile*

(Received 8 September 2021; revised 29 November 2021; accepted 28 February 2022; published 15 March 2022)

In a hybrid scheme, consisting of a three-level atom-cavity-oscillator system, we show that synchronization [J. Czartowski, R. Müller, K. Życzkowski, and D. Braun, *Phys. Rev. A* **104**, 012410 (2021)] and transfer of nonclassical states between the mechanical oscillator and the cavity field is possible. In this framework, we show that an initially thermalized mechanical oscillator, when connected to a squeezed bath, evolves to a squeezed state which in steady state is synchronized with the cavity mode. On the other hand, if the mechanical oscillator is initially prepared in a nonclassical state, e.g., squeezed and Schrödinger's cat states, while the cavity is in a thermal state, then a periodic transfer between the mechanical oscillator and cavity mode occurs for given interaction times. As qualitative results, we prove that the synchronization and transfer of the quantum states are feasible with high fidelity.

DOI: [10.1103/PhysRevA.105.033708](https://doi.org/10.1103/PhysRevA.105.033708)**I. INTRODUCTION**

With the remarkable state of the art of hybrid systems [1–3] composed of mechanical oscillators (MO), cavities, spins, etc., it is becoming more and more feasible to control such systems in their quantum regime in the search for nonclassical features of their elements. Besides MO have the ability to easily interact with a wide range of physical systems, such as ultracold atomic Bose-Einstein condensates (BECs) [4], superconducting qubits [3], spin states in quantum dots [5,6] and color and nitrogen-vacancy (NV) centers [2,7,8], cavity fields in optomechanical systems [9,10], etc. Actually, the cooling down to subkelvin temperatures of relatively large mechanical objects can be reached through different techniques such as feedback cooling [11,12] and dynamical decoupling in spin mechanics [7,13], allowing the mechanical system to oscillate with very low number of quanta excitations that is useful for different applications in the framework of the hybrid devices. The aforementioned hybrid mechanical architectures are acquiring increasing attention in order to understand the foundations of quantum theory, such as macroscopic quantum superpositions [14–17] and quantum correlations at macroscopic scales [9,18]—very well-known questions of quantum mechanics since Schrödinger's times.

The hybrid setups are of paramount importance regarding the development of quantum technologies. Therefore, to move

forward the limits of fields such as quantum computing, quantum networks, and quantum metrology and sensing, a very desirable tool should be the high-fidelity transfer of the quantum states between the components of a hybrid system. For instance, in the realm of quantum networks, the mechanical object can serve as light-matter transducer [19,20] or to map or encode information from a qubit [3,21]. Particularly, spin-mechanical systems have attained major attention, mainly because spin systems exhibit long-coherence times and they can be easily manipulated and read out [13,22]. A rapidly emerging field is quantum metrology and sensing [23] by using the quantum states and protocols with the aim to obtain precision unreachable by classical sensing. There are several experiments proving sensing near and beyond the standard quantum limit, e.g., [24–26]. Nevertheless, quantum metrology needs more elaborate techniques and methods in order to improve the precision from shot noise to the Heisenberg limit. Commonly quantum sensors are based on photonics setups, involving cavities, atoms, photons, trapped ions, and solid-state systems with electrons, superconducting junctions, etc. Nevertheless, hybrid systems like opto- or spin-mechanical, opto-electromechanical setups, etc., actually become more attractive for their effectiveness and usefulness for a wide range of quantum applications, from gravitational wave detectors [27,28] to force microscopes [29,30], hence they are considered leading candidates for quantum metrology and sensing.

In this context, the squeezing of the modes in a hybrid system, and particularly the squeezing transfer between them, is of major importance and applicability. On the one hand, the preparation of the mechanical and light modes in the squeezed states has been widely investigated theoretically [31–34] and

<sup>\*</sup>hugo.molinares@mayor.cl<sup>†</sup>vitalie.ereemeev@udp.cl<sup>‡</sup>Corresponding author: miguel.orszag@umayor.cl

is nowadays experimentally feasible in versatile hybrid setups [10,35–40].

On the other hand, as far as we know, there are fewer proposals for the effect of dynamical synchronization of quantum states, particularly in hybrid systems. By dynamical synchronization we mean a high-fidelity transfer of the quantum stationary state from one subsystem to another one and keeping both subsystems in the same state for as long a time as possible under the effects of decoherence. This synchronization is dynamically irreversible (cannot return to the initial state) as the system reaches steady state when connected to noisy channels. From a practical point of view, such an effect may be useful for long time storage or protection of the quantum information [17] for different degrees of freedom, and further the quantum state can be transferred, for example by another protocol, to a quantum network. The concept of quantum-state synchronization as a general procedure was recently proposed in [41] and our work can be regarded as a practical realization of this idea in an atom-optomechanical setup. The models developed in [42–44] can be considered similar to quantum state synchronization. Another kind of quantum-state transfer we propose here is the periodic reversible transfer of the squeezed and Schrödinger cat states between the MO and cavity modes, realized at high fidelity as well. The protocols of periodic transfer as compared to the synchronization are more common and have been investigated for a variety of configurations [45–47].

Therefore, in the present work we propose the optomechanical protocols of high-fidelity squeezing synchronization and transfer of quantum states between the mechanical and cavity modes. Our results show that a squeezing synchronization can be realized with the system coupled to a squeezed phononic bath, in order to get steady state squeezing of the photons in the cavity. As well, we prove that the transfer of squeezed or cat states between the MO and cavity modes occurs with some periodicity during the interaction. These effects are realizable in the regime of weak optomechanical coupling; however the fidelity can be improved by enhancing the optomechanical and Jaynes-Cummings couplings and reducing the loss rates, which is technologically attainable nowadays.

## II. MODEL

Consider a hybrid atom-cavity-mechanics system, as illustrated in panel (a) of Fig. 1. The Jaynes-Cummings type interaction between the two upper levels of the three-level atom and the mode of the electromagnetic field of frequency  $\omega_c$  is quantified by the coupling constant  $g_{ac}$ . The interaction between the cavity and the MO of frequency  $\omega_m$  corresponds to the standard optomechanical coupling and is quantified by the coupling constant  $g_{cm}$ .

The hybrid system is described by the Hamiltonian under the rotating wave approximation as ( $\hbar = 1$ )

$$\mathcal{H} = \sum_{i=0}^2 \omega_i \sigma_{ii} + \omega_c a^\dagger a + \omega_m b^\dagger b + i g_{ac} (a \sigma_{21}^+ - a^\dagger \sigma_{21}^-) - i g_{cm} a^\dagger a (b^\dagger - b), \quad (1)$$

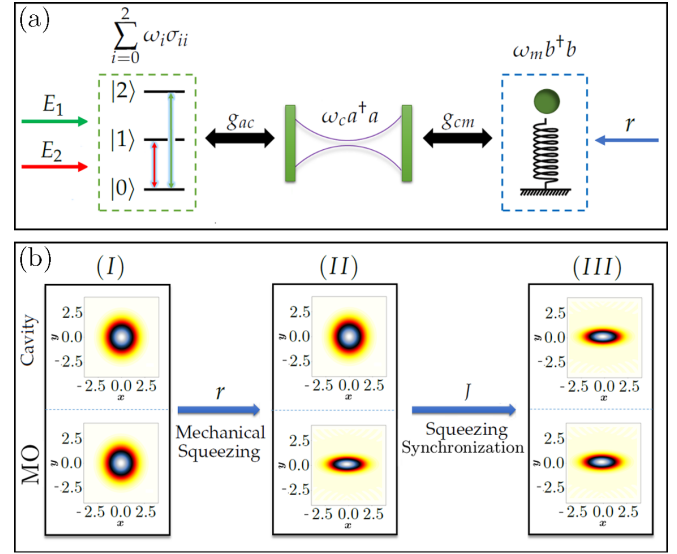


FIG. 1. (a) Schematic diagram of a hybrid cavity-atom-mechanics system. (b) Visualization of the Wigner function to explain how the MO is dynamically squeezed and the cavity mode is synchronized to this squeezing in the steady state.

where  $\omega_i$  are the energy levels of the three-level atom.  $a$  ( $a^\dagger$ ) and  $b$  ( $b^\dagger$ ) are the annihilation (creation) operators of the cavity and the MO, respectively. The atomic operators of lowering (raising) are denoted as  $\sigma_{ij}^-$  ( $\sigma_{ij}^+$ ) =  $|i\rangle\langle j|$  ( $|j\rangle\langle i|$ ), and obey standard anticommutation relations.

In the following, we calculate the full Hamiltonian in the interaction picture (rotating at the mechanical frequency  $\omega_m$ ) taking the form (see details in Appendix A)

$$\tilde{\mathcal{H}}_1 = i g_{ac} \sigma_{21}^+ a e^{i\Delta t} e^{-iF^*(t)} + \text{H.c.} \quad (2)$$

Here we used the Hermitian operator  $F \equiv \frac{g_{cm}}{\omega_m} (b^\dagger \eta^* + b \eta)$ , with  $\eta \equiv e^{i\omega_m t} - 1$ ;  $\Delta \equiv \omega_2 - \omega_1 - \omega_c$  is the detuning.

Considering the experiments in optomechanics [1] we assume that the optomechanical coupling  $g_{cm}$  is much smaller than the mechanical frequency  $\omega_m$ , so that  $e^{-iF^*(t)} \approx 1 - i \frac{g_{cm}}{\omega_m} (b^\dagger \eta^* + b \eta)$ . Then we have

$$\tilde{\mathcal{H}}_2 = iJ (\sigma_{21}^+ a b^\dagger - \sigma_{21}^- a^\dagger b), \quad (3)$$

where  $J \equiv g_{ac} \times g_{cm} / \omega_m$  is the tripartite atom-photon-phonon interaction strength.

To obtain Eq. (3) we considered the blue-detuned regime  $\Delta = \omega_m$  that selects two possible processes: (i) a phonon is absorbed, the atom decays from state  $|2\rangle$  to  $|1\rangle$ , and a photon is created; and (ii) a phonon is created, the atom is excited from state  $|1\rangle$  to  $|2\rangle$ , and a photon is absorbed. In addition, we have considered the rotating wave approximation and ignored high frequency terms (See details in Appendix A).

### A. Theoretical framework in the presence of driving and dissipation

In this section, we explain how to produce squeezed light in the optical cavity through different types of driving applied in the main model developed in the previous section. For this, we can follow the sequence shown in panel (b) of the

Fig. 1. Initially (I) the states of the cavity field and MO are in vacuum states, and subsequently (II) the MO is squeezed via its coupling to the squeezed reservoir,  $\mathcal{L}_{sq}[b]$  (as explained below).

Additionally two lasers  $E_1$  and  $E_2$  (proportional to the field strengths) are introduced in the system, and are resonant with the transitions of the levels  $|2\rangle \longleftrightarrow |0\rangle$  and  $|1\rangle \longleftrightarrow |0\rangle$ , respectively [see panel (a) of Fig. 1]. These coherent drives are described by the Hamiltonian in the interaction picture,

$$\tilde{\mathcal{H}}_E = iE_1(\sigma_{20}^- - \sigma_{20}^+) + iE_2(\sigma_{10}^- - \sigma_{10}^+). \quad (4)$$

Assuming that the  $|1\rangle \longleftrightarrow |0\rangle$  transition (coupled to the classical field  $E_2$ ) and the  $|2\rangle \longleftrightarrow |1\rangle$  transition (coupled to the quantum field) are dipole allowed, that is, of opposite parity, then the driving field  $E_1$  will necessarily couple to the  $|2\rangle \longleftrightarrow |0\rangle$  transition, whose states have the same parity and are thus dipole forbidden. To be able to achieve this coupling, we can use a nonlinear process as an effective coherent pump from a Raman type configuration resonant to the carrier transition where a fourth level was present and adiabatically eliminated. Basically, the role of each laser is quite different:  $E_1$  populates level  $|2\rangle$  to keep the creation of photons, while  $E_2$  is necessary to transfer the coherence from the mechanical oscillator state to the cavity field.

If we now include the dissipation caused by the system-environment coupling, the dissipative dynamics of the hybrid quantum system is described by the Markovian master equation (ME) for the the density matrix as follows:

$$\begin{aligned} \frac{d\rho}{dt} = & -i[\tilde{\mathcal{H}}_2 + \tilde{\mathcal{H}}_E, \rho] + \frac{\gamma_{21}}{2}\mathcal{L}[\sigma_{21}^-]\rho \\ & + \frac{\gamma_{10}}{2}\mathcal{L}[\sigma_{10}^-]\rho + \frac{\kappa_a}{2}\mathcal{L}[a]\rho + \frac{\kappa_b}{2}\mathcal{L}_{sq}[b]\rho, \end{aligned} \quad (5)$$

where the common Lindblad dissipative terms are defined as follows:  $\forall \mathcal{O}$ ,  $\mathcal{L}[\mathcal{O}] = 2\mathcal{O}\rho\mathcal{O}^\dagger - \mathcal{O}^\dagger\mathcal{O}\rho - \rho\mathcal{O}^\dagger\mathcal{O}$ , with all the baths at  $n_{th} = 0$ . Here  $\gamma_{21}$  ( $\gamma_{10}$ ) corresponds to spontaneous emission rate from level 2 to 1 (level 1 to 0), and  $\kappa_a$  ( $\kappa_b$ ) is the decay rate of the optical (mechanical) mode. Additionally, the Lindbladian corresponding to the squeezed phononic bath reads  $\mathcal{L}_{sq}[b] = (N_{sq} + 1)(2b\rho b^\dagger - b^\dagger b\rho - \rho b^\dagger b) + N_{sq}(2b^\dagger\rho b - bb^\dagger\rho - \rho bb^\dagger) + M_{sq}(2b^\dagger\rho b^\dagger - b^\dagger b^\dagger\rho - \rho b^\dagger b^\dagger) + M_{sq}^*(2b\rho b - bb\rho - \rho bb)$ ; here  $N_{sq} = \sinh^2 r$  corresponds to the average number of phonons in the squeezed bath at zero temperature and the quantity  $M_{sq} = -\exp(i\theta)\sinh r \cosh r$  obeys the relation  $|M_{sq}| = \sqrt{N_{sq}(N_{sq} + 1)}$ . Here the parameters  $r$  and  $\theta$  represent the squeezing amplitude and the phase, respectively, as they appear in the definition of the complex squeezing parameter,  $\xi = r \exp[i\theta]$ .

### III. STEADY-STATE SYNCHRONIZATION OF SQUEEZING IN MECHANICAL AND CAVITY MODES

After building the theoretical framework of the model, we discuss the degree of squeezing present in the states of the cavity and the MO. For this, we rely on numerical methods according to [48] to solve Eq. (5) in the steady state, i.e.,  $\dot{\rho} = 0$ , and so calculate the quadrature fluctuations defined by

$$(\Delta x_{\mathcal{O}=a,b})^2 = \langle ([\mathcal{O}e^{-i\phi} + \mathcal{O}^\dagger e^{i\phi}]/2)^2 \rangle, \quad (6)$$

$$(\Delta y_{\mathcal{O}=a,b})^2 = \langle ([\mathcal{O}e^{-i\phi} - \mathcal{O}^\dagger e^{i\phi}]/2i)^2 \rangle, \quad (7)$$

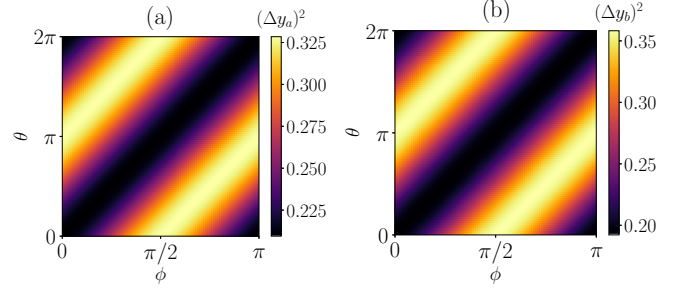


FIG. 2. Quadrature fluctuations (a)  $(\Delta y_a)^2$  and (b)  $(\Delta y_b)^2$  as functions of the phase  $\theta$ , characterizing the squeezed bath, and the phase,  $\phi$ , defining the direction of the axes of squeezing as in Eq. 7. The parameters (in units of  $\omega_m$ ) are:  $g_{ac} = 10^2$ ,  $g_{cm} = 0.01$ ,  $\kappa_a = \kappa_b = 0.2$ ,  $\gamma_{01} = 20$ ,  $\gamma_{21} = 0$ ,  $r = 0.3$ ,  $E_1 = E_2 = 25$ . Both fields reach the minimum fluctuations for the same values, e.g.  $\{\phi, \theta\} = \{(0, 0), \{\pi/2, \pi\}, \{\pi, 0\}, \dots\}$

where  $\phi$  permits us to generalize the direction of the quadrature fluctuations; i.e., it indicates the squeezing along any pair of axes ( $x'$ ,  $y'$ ) in the phase space. In order to minimize the fluctuations and achieve an optimal squeezing synchronization in the stable region, we chose one set of values as  $\{\phi, \theta\} = \{0, 0\}$ ; see Fig. 2. For a better understanding the synchronization effect and stability of the hybrid system, we get a set of first-order differential equations from Eq. (5):

$$\frac{d\langle a^\dagger a \rangle}{dt} = -2J\langle a^\dagger b \rangle \langle \sigma_{21}^- \rangle - \kappa_a \langle a^\dagger a \rangle, \quad (8)$$

$$\frac{d\langle b^\dagger b \rangle}{dt} = 2J\langle a^\dagger b \rangle \langle \sigma_{21}^- \rangle - \kappa_b \langle b^\dagger b \rangle + \kappa_b N_{sq}, \quad (9)$$

$$\frac{d\langle a^2 \rangle}{dt} = -2J\langle ab \rangle \langle \sigma_{21}^- \rangle - \kappa_a \langle a^2 \rangle, \quad (10)$$

$$\frac{d\langle b^2 \rangle}{dt} = 2J\langle ab \rangle \langle \sigma_{21}^+ \rangle - \kappa_b \langle b^2 \rangle - \kappa_b M_{sq}, \quad (11)$$

$$\begin{aligned} \frac{d\langle a^\dagger b \rangle}{dt} = & -J(\langle b^\dagger b \rangle \langle \sigma_{21}^+ \rangle - \langle a^\dagger a \rangle \langle \sigma_{21}^+ \rangle) \\ & - \frac{\kappa_a}{2} \langle a^\dagger b \rangle - \frac{\kappa_b}{2} \langle a^\dagger b \rangle, \end{aligned} \quad (12)$$

$$\begin{aligned} \frac{d\langle ab \rangle}{dt} = & -J(\langle b^2 \rangle \langle \sigma_{21}^- \rangle - \langle a^2 \rangle \langle \sigma_{21}^+ \rangle) \\ & - \frac{\kappa_a}{2} \langle ab \rangle - \frac{\kappa_b}{2} \langle ab \rangle, \end{aligned} \quad (13)$$

where we have considered the factorization of the form  $\langle a^\dagger b \sigma_{21}^- \rangle = \langle a^\dagger b \rangle \langle \sigma_{21}^- \rangle$ , thereby neglecting the quantum fluctuations between the boson and atomic operators, i.e., a semiclassical approximation. In order to confirm the validation of such approximation, we compare the analytical solutions for the quadrature fluctuations with the numerical solution of the master equation (5). Therefore, the results in Fig. 3(a) show clearly that the semiclassical approximation is successfully validated in the range of low values of the squeezing parameter,  $r$ . By considering  $\{E_1, E_2, \gamma_{10}\} \gg \{J, \kappa_a, \kappa_b\}$  and  $\gamma_{21} = 0$ , we get the following semiclassical results for

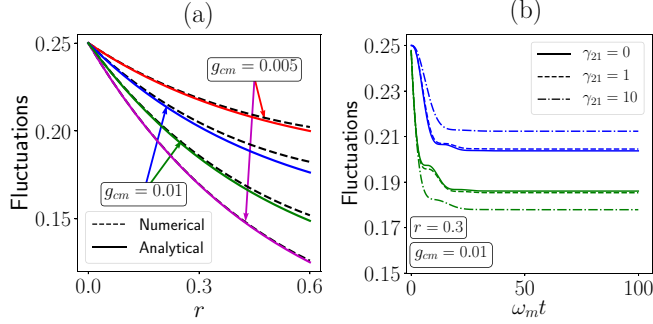


FIG. 3. (a) Quadrature fluctuations for photons,  $(\Delta y_a)^2$  (red and blue line), and phonons,  $(\Delta y_b)^2$  (green and magenta line), as functions of the parameter  $r$  for different optomechanical couplings and  $\gamma_{21} = 0$ . Here we compare: (i) analytical solutions, Eqs. 14–15 (dashed) and (ii) numerical solution of the ME (5) (solid line). (b) Numerical results of the fluctuations vs. time, evidencing the steady-state for different  $\gamma_{21}$ . The parameters (in units of  $\omega_m$ ) are the same as in Fig. 2 with  $\theta = 0$  and  $\phi = 0$ .

the quadrature fluctuations in steady state (see details in Appendix B):

$$(\Delta y_a)^2 = \frac{1}{4}p + l, \quad (14)$$

$$(\Delta y_b)^2 = \frac{1}{4}p[2(N_{sq} + M_{sq}) + 1] + l, \quad (15)$$

where

$$l = \frac{J^2 \langle \sigma_{21}^+ \rangle^2 [\kappa_b(1 + 2[N_{sq} + M_{sq}]) + \kappa_a]}{(\kappa_a + \kappa_b)(4J^2 \langle \sigma_{21}^+ \rangle^2 + \kappa_a \kappa_b)}, \quad (16)$$

$$p = \frac{\kappa_a \kappa_b}{(4J^2 \langle \sigma_{21}^+ \rangle^2 + \kappa_a \kappa_b)}. \quad (17)$$

In panel (a) of Fig. 3 the quadrature fluctuations are presented as functions of the parameter  $r$  using both the analytical results [Eqs. (14) and (15)] as well as numerical calculations based on the Hamiltonian given by Eq. (5). The results show that for  $g_{cm} = 0.01$  the synchronization is performed optimally; i.e., since the curves are closer, the fluctuations are similar. In panel (b) of Fig. 3, we show the time evolution of the quadrature fluctuations. Without loss of generality, we have fixed the parameters  $r = 0.3$  and  $g_{cm} = 0.01$ . As a result of this analysis, one sees how the interaction with a squeezed bath of MO leads to mechanical and cavity squeezing in steady state.

#### A. Feasible synchronization via the optomechanical coupling

To achieve the optimal synchronization we need to study the parameters in our hybrid system in which quadrature fluctuations reach their minimum values. To illustrate the differences between optical and mechanical states, we numerically investigate effect of synchronization in the steady state of our model, computing the fidelity  $\mathcal{F}$ , defined as the overlap between the final mechanical and cavity states. The fidelity is defined by [49]

$$\mathcal{F}(\rho_c^{ss}, \rho_m^{ss}) \equiv \text{Tr} \sqrt{\sqrt{\rho_c^{ss}} \rho_m^{ss} \sqrt{\rho_c^{ss}}}, \quad (18)$$

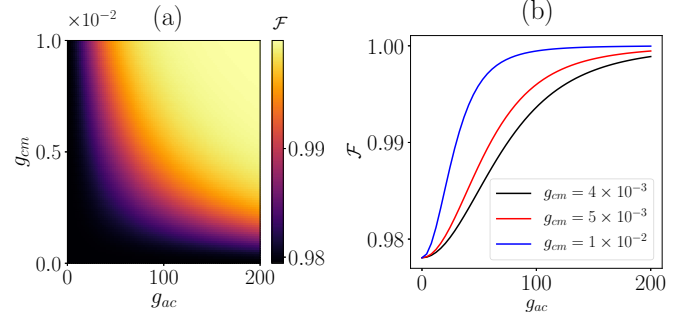


FIG. 4. (a) Fidelity of squeezing synchronization between the mechanical and cavity modes as a function of the couplings  $g_{cm}$  and  $g_{ac}$ . (b) Fidelity as a function of  $g_{ac}$  for some couplings  $g_{cm}$ . The fidelity is close to unity as the optomechanical and Jaynes-Cummings couplings increase. The parameters (in units of  $\omega_m$ ) are the same as in Fig. 3 with  $r = 0.3$ .

where  $\rho_c^{ss}$  and  $\rho_m^{ss}$  are the density operators of the cavity and mechanical modes in the steady state. In panel (a) of Fig. 4 we show the fidelity as a function of  $g_{cm}$  and  $g_{ac}$ . Notice that the fidelity is close to unity as the optomechanical and Jaynes-Cummings couplings increase, even in the presence of dissipation in the system. In panel (b) of Fig. 4 we show the fidelity as a function of  $g_{ac}$  for some values of  $g_{cm}$ . This result allows us to conclude that in the strong coupling regime the open system allows the squeezing synchronization with a reliability close to 100%.

## IV. DYNAMICAL TRANSFER OF QUANTUM STATES

In this section, we show that a mechanical nonclassical state can be transferred to the photons in the cavity at certain times and given an initial preparation of both states. Taking the model under study explained in Sec. II and using only atomic pumps of the type  $\mathcal{H}_E$ , we numerically develop the study of transfer of squeezed and cat-type states.

### A. Squeezed state transfer

We assume the MO to be initially prepared in a squeezed state [10,38,39] given by

$$|\psi(0)\rangle_m = S(\xi)|0\rangle, \quad (19)$$

where

$$S(\xi) = \exp\left[\frac{1}{2}(\xi^* b^2 - \xi b^{\dagger 2})\right] \quad (20)$$

is a unitary transformation and  $\xi = r \exp(i\theta)$  is the squeeze parameter. Whereas the state of the cavity field is assumed initially to be in a thermal state, that in the coherent basis can be written as

$$\rho_c(0) = \frac{1}{\pi \bar{n}} \int |\alpha\rangle \langle \alpha| e^{-\frac{|\alpha|^2}{\bar{n}}} d^2 \alpha, \quad (21)$$

where  $\bar{n} = \{\exp[\omega_c/(\kappa_b T)] - 1\}^{-1}$ , is the average value of photon occupation number and  $\kappa_b$  is Boltzmann's constant.

Now, for the study of the transfer, both states are submitted to the kernel given by  $\tilde{\mathcal{H}}_2 + \tilde{\mathcal{H}}_E$  (see Fig. 5). The dynamics of the system subjected to different types of losses—atomic,

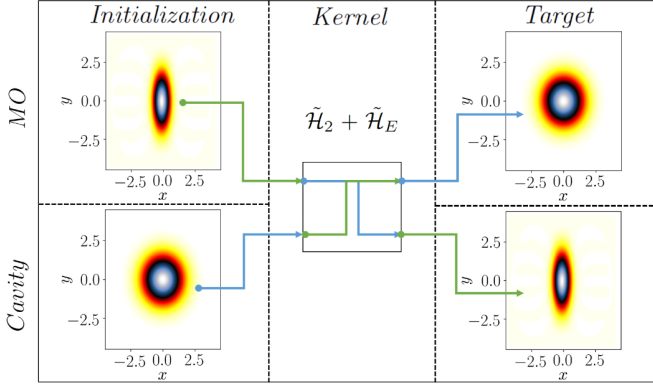


FIG. 5. Scheme for transfer of nonclassical states (squeezing and cat states). The MO initialized in a nonclassical state and a thermal state in the cavity are subjected to kernel  $\tilde{\mathcal{H}}_2 + \tilde{\mathcal{H}}_E$  generating a complete transfer of the initial states in the target.

mechanical, and of the cavity—is governed by the master equation

$$\begin{aligned} \frac{d\rho}{dt} = & -i[\tilde{\mathcal{H}}_2 + \tilde{\mathcal{H}}_E, \rho] + \frac{\gamma_{21}}{2}\mathcal{L}[\sigma_{21}^-]\rho \\ & + \frac{\gamma_{10}}{2}\mathcal{L}[\sigma_{10}^-]\rho + \frac{\kappa_a}{2}\mathcal{L}[a]\rho + \frac{\kappa_b}{2}\mathcal{L}[b]\rho, \end{aligned} \quad (22)$$

In Fig 6, we calculate the Wigner functions of the mechanical oscillator and cavity fields for a lossless case, observing the transfer from one mode to the other one after a given time,  $t = 2\pi/\omega_m$ . In order to quantify the feasibility of the state transfer, in the following we will use the fidelity function, similarly as in the synchronization effect.

### B. Schrödinger's cat state transfer

Following the scheme shown in the previous subsection (see Fig. 5), here it is shown that the transfer can also occur for cat-type [16,17] entries. To do this, we initialize the

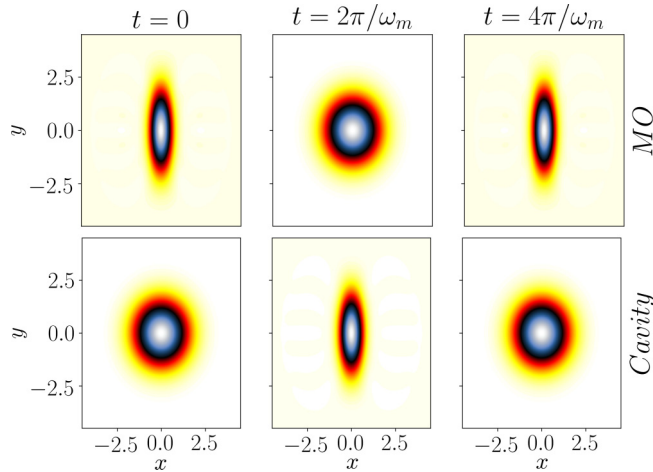


FIG. 6. Wigner function visualization of the transfer from a squeezed mechanical state (upper panel) to the cavity field (lower panel). The other parameters (in units of  $\omega_m$ ) are  $g_{ac} = 10^2$ ,  $g_{cm} = 0.01$ ,  $\kappa_a = \kappa_b = 0$ ,  $\gamma_{10} = 0$ ,  $\gamma_{21} = 0$ ,  $E_1 = E_2 = 100$ ,  $\xi = 0.5$ , and  $\bar{n} = 0.5$ .

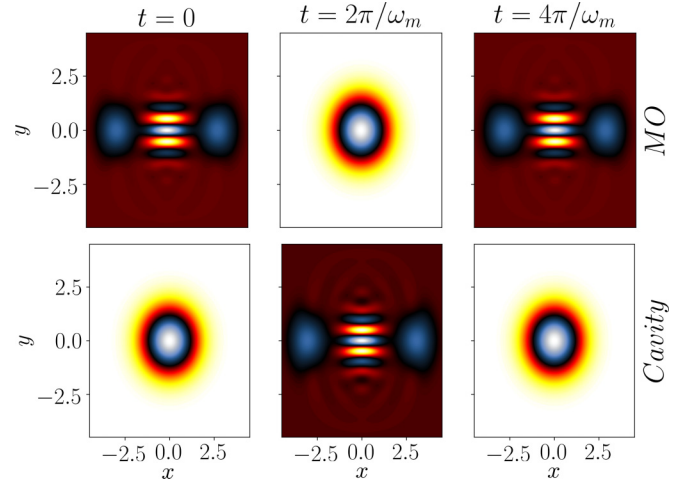


FIG. 7. Wigner function visualization of the transfer of a mechanical cat state (upper panel) to the cavity field (lower panel). The other parameters (in units of  $\omega_m$ ) are  $g_{ac} = 10^2$ ,  $g_{cm} = 0.01$ ,  $\kappa_a = \kappa_b = 0$ ,  $\gamma_{10} = 0$ ,  $\gamma_{21} = 0$ ,  $E_1 = E_2 = 100$ ,  $\bar{n} = 0.5$ , and  $\alpha = 2$ .

mechanical state of the form

$$|\psi(0)\rangle_m = \mathcal{N}(|\alpha\rangle + |-\alpha\rangle) \quad (23)$$

where  $\mathcal{N}$  is a normalization constant. The cavity field is initially assumed to be in a thermal state [Eq. (21)]. In Fig. 7 it is shown that the cavity field achieves the cat state transfer for  $\omega_m t = 2\pi$  and with the same periodicity as for the transfer of squeezing. We use the measure of fidelity as a figure of merit to quantify the degree of transfer of states during their evolution, which is defined as

$$F(\rho_m(0), \rho_c(t)) \equiv \text{Tr} \sqrt{\sqrt{\rho_m(0)}\rho_c(t)\sqrt{\rho_m(0)}}. \quad (24)$$

The above definition shows that the measurement is made between the initial state of MO and the state of the cavity during its evolution.

Therefore, in Fig. 8 we show the fidelity of transferring the quantum states as squeezed (a) and Schrödinger's cat

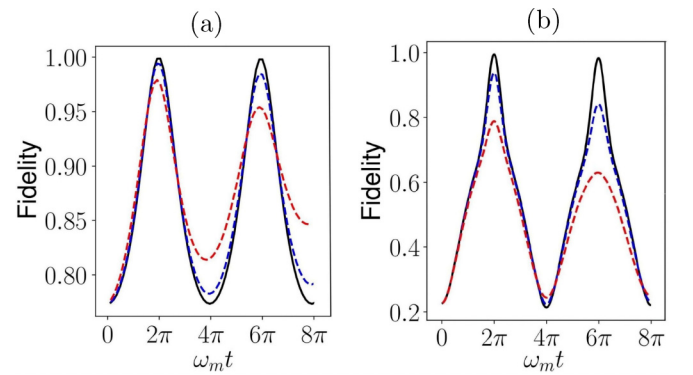


FIG. 8. Fidelity of transferring from the MO to the cavity field: (a) a squeezed state (with  $\xi = 0.5$ ) and (b) a cat state (with  $\alpha = 2$ ). For situations: no losses (black line), losses with  $\gamma_{21} = \gamma_{10} = \kappa_a = 0.01$ ,  $\kappa_b = \kappa_a/100$  (blue line), and losses with  $\gamma_{21} = \gamma_{10} = \kappa_a = 0.05$ ,  $\kappa_b = \kappa_a/100$  (red line). The other parameters (in units of  $\omega_m$ ) are:  $g_{ac} = 10^2$ ,  $g_{cm} = 0.01$ ,  $E_1 = E_2 = 100$  and  $\bar{n} = 0.5$ .

(b) between the mechanical and the cavity modes. It can be seen that the fidelity is close to its maximum value for the lossless system (black line). However, for the hybrid system with losses, the transfer is not perfect (red and blue lines), where one observes the optimal state transfer for  $t = 2\pi/\omega_m$  and after each period of  $4\pi$  the fidelity decreases.

## V. CONCLUDING REMARKS

In summary, we have proposed a hybrid system consisting of a three-level atom, an optical cavity, and a mechanical resonator that allows the steady-state squeezing synchronization. We demonstrated that by considering the hybrid system connected to a bath of squeezed phonons and also adding two coherent atomic drives, one can synchronize a steady-state squeezing in the mechanical and cavity modes at high fidelity, close to unity (see Fig. 4). It is important to remark that the synchronization effect in our model occurs only under the blue detuned regime, i.e.,  $\Delta = \omega_m$ . For a qualitative description of how the squeezing is synchronized, one gets the sequence of processes from the initial state, where an arbitrary state is defined as  $|n_s, n_a, n_b\rangle$  ( $n_s, n_a, n_b$  label the excitation numbers in atom, cavity, and oscillator, respectively):

$$\begin{aligned} |000\rangle &\xrightarrow{E_1} |200\rangle \xrightarrow{r} |202\rangle \xrightarrow{J} |111\rangle \\ &\xrightarrow{E_2} |011\rangle \xrightarrow{E_1} |211\rangle \xrightarrow{J} |120\rangle \xrightarrow{r} |122\rangle, \end{aligned}$$

where we have chosen the process  $\sigma^- a^\dagger b + \text{H.c.}$ . In the previous sequence, it can be seen that the occupational number for the cavity field and mechanical oscillator ends with a pair of photons and phonons (presence of squeezed state). On the other hand, if we go to the red detuned regime, i.e.,  $\Delta = -\omega_m$ , the corresponding sequence leads to an amplification effect:

$$\begin{aligned} |000\rangle &\xrightarrow{E_1} |200\rangle \xrightarrow{r} |202\rangle \xrightarrow{J} |113\rangle \\ &\xrightarrow{E_2} |013\rangle \xrightarrow{E_1} |213\rangle \xrightarrow{J} |124\rangle \xrightarrow{r} |126\rangle. \end{aligned}$$

This last effect is not relevant in this study, but it may be a motivation to explore effects such as radiation-pressure-driven optomechanical parametric amplification [50,51]. As for experimental applications, it is important to mention that by increasing the optomechanical coupling one gets better results in producing closer phonon and photon squeezed states, i.e., improving the protocol of synchronization. Moreover, we highlight that the ‘‘synchronization’’ process is clearly irreversible, since the system is subject to losses throughout the process in which it reaches a stationary state, so that it is not possible to return to the initial state in this scheme. In addition, we present another scheme that allows reversibility in the transferring of states. In this case, we show (for negligible losses), at specific interaction times, a possibility of transfer of quantum states, that is from an initial squeezed or cat vibrational state to the cavity or vice versa, by using the model under study (see results in Sec. IV). The parameters used in this work are compatible with recent experiments using optomechanical hybrid setups, e.g., [1]. The proposed protocols of high-fidelity synchronization and periodic transfer of the squeezing and Schrödinger cats, between the mechanical and cavity modes in a hybrid system, attest to the novelty of this

work, thereby contributing to the state of the art of the field of optomechanics.

As a matter of fact, in a very recent study [41], an experiment of quantum state synchronization is simulated on the five-qubit IBM quantum computer. For this simulation, the authors demonstrate the synchronization of a quantum state in a two-qubit circuit with one ancillary qubit. As well, in such an experiment the quantum hardware’s imperfection is witnessed as asynchronicity.

## ACKNOWLEDGMENTS

H.M. acknowledges financial support from Universidad Mayor through a doctoral fellowship. V.E. and M.O. acknowledge financial support from Fondecyt Regular No. 1180175.

## APPENDIX A: ANALYTICAL MODEL

In this Appendix, we provide the derivation of the Hamiltonian in the interaction picture used as a theoretical model. Initially, we calculate a Hamiltonian in the first interaction picture, that is

$$\mathcal{V} = e^{i\mathcal{H}_0 t} \mathcal{H}_I e^{-i\mathcal{H}_0 t}, \quad (\text{A1})$$

where we have defined the quantities

$$\mathcal{H}_0 = \sum_{i=0}^2 \omega_i \sigma_{ii} + \omega_c a^\dagger a + \omega_m b^\dagger b, \quad (\text{A2})$$

$$\mathcal{H}_I = ig_{ac}(a\sigma_{21}^+ - a^\dagger \sigma_{21}^-) - ig_{cm} a^\dagger a(b^\dagger - b). \quad (\text{A3})$$

From Eq. (A1), we readily get

$$\begin{aligned} \mathcal{V} &= ig_{ac}(\sigma_{21}^+ a e^{i\Delta t} - \sigma_{21}^- a^\dagger e^{-i\Delta t}) \\ &\quad - ig_{cm} a^\dagger a(b^\dagger e^{i\omega_m t} - b e^{-i\omega_m t}), \end{aligned} \quad (\text{A4})$$

where  $\Delta = \omega_2 - \omega_1 - \omega_c$ .

Now, we move on to a second interaction picture, defined as (for  $g_{cm}/\omega_m \ll 1$ )

$$\tilde{\mathcal{H}}_1 = \exp\left\{i \int \mathcal{V}_0 dt\right\} \mathcal{V}_I \exp\left\{-i \int \mathcal{V}_0 dt\right\}, \quad (\text{A5})$$

where

$$\mathcal{V}_0 = -ig_{cm} a^\dagger a(b^\dagger e^{i\omega_m t} - b e^{-i\omega_m t}), \quad (\text{A6})$$

$$\mathcal{V}_I = ig_{ac}(\sigma_{21}^+ a e^{i\Delta t} - \sigma_{21}^- a^\dagger e^{-i\Delta t}), \quad (\text{A7})$$

readily getting

$$\tilde{\mathcal{H}}_1 = ig_{ac}(\sigma_{21}^+ a e^{i\Delta t} e^{-iF^*(t)} - \sigma_{21}^- a^\dagger e^{-i\Delta t} e^{iF(t)}), \quad (\text{A8})$$

where we have introduced a Hermitian operator  $F(t) = \frac{g_{cm}}{\omega_m}(b^\dagger \eta^* + b\eta)$  with  $\eta = e^{i\omega_m t} - 1$ . We notice that the  $\exp[iF(t)]$  term in Eq. (A8) corresponds to mechanical displacement operators.

### 1. Approximation $g_{cm} \ll \omega_m$

Here, we assume the optomechanical coupling  $g_{cm}$  is much smaller than the mechanical frequency  $\omega_m$ , so that  $e^{-iF^*(t)} \approx 1 - i \frac{g_{cm}}{\omega_m}(b^\dagger \eta^* + b\eta)$ . Thus

$$\begin{aligned} \tilde{\mathcal{H}}_2 &= ig_{ac}(\sigma_{21}^+ a e^{i\Delta t} - \sigma_{21}^- a^\dagger e^{-i\Delta t}) \\ &\quad + J(\sigma_{21}^+ a b^\dagger e^{i(\Delta - \omega_m)t} - \sigma_{21}^- a b^\dagger e^{i\Delta t}) \end{aligned}$$

$$\begin{aligned}
& + \sigma_{21}^+ a b e^{i(\Delta+\omega_m)t} - \sigma_{21}^+ a b e^{i\Delta t} \\
& + J(\sigma_{21}^- a^\dagger b^\dagger e^{-i(\Delta+\omega_m)t} - \sigma_{21}^- a^\dagger b^\dagger e^{-i\Delta t}) \\
& + \sigma_{21}^- a^\dagger b e^{-i(\Delta-\omega_m)t} - \sigma_{21}^- a^\dagger b e^{-i\Delta t}. \quad (\text{A9})
\end{aligned}$$

Now, by applying the unitary operator  $\mathcal{U} = \exp(-i\chi a^\dagger a)$  with  $\chi = \pi/2$  and considering the blue detuned regime  $\Delta = \omega_m$ , the above equation leads to (keeping only the time independent terms)

$$\tilde{\mathcal{H}}_2 = iJ(\sigma_{21}^+ a b^\dagger - \sigma_{21}^- a^\dagger b). \quad (\text{A10})$$

## APPENDIX B: DETERMINATION OF THE MOMENTS $\langle a^\dagger a \rangle$ , $\langle b^\dagger b \rangle$ , $\langle a^2 \rangle$ , AND $\langle b^2 \rangle$

In this Appendix, to study the synchronization effect, we analytically solve the quadrature fluctuations [Eq. (7)] and for this we need to determine the quantities  $\langle a^\dagger a \rangle$ ,  $\langle b^\dagger b \rangle$ ,  $\langle a^2 \rangle$ , and  $\langle b^2 \rangle$ .

As the set of equations (8)–(13) is not closed, in order to obtain all the moments for the bosonic operators, it is necessary to build another set of equations. For this purpose, we take the equations for the atomic moments in the semiclassical approximation:

$$\begin{aligned}
\frac{d\langle \sigma_{21}^\dagger \rangle}{dt} & = J\langle a^\dagger b \rangle \langle \sigma_{21}^\dagger \rangle - E_1 \langle \sigma_{10}^- \rangle - E_2 \langle \sigma_{20}^+ \rangle \\
& - \frac{\gamma_{21}}{2} \langle \sigma_{21}^+ \rangle - \frac{\gamma_{10}}{2} \langle \sigma_{21}^+ \rangle, \quad (\text{B1})
\end{aligned}$$

$$\frac{d\langle \sigma_{10}^\dagger \rangle}{dt} = J\langle a^\dagger b \rangle \langle \sigma_{20}^+ \rangle + E_1 \langle \sigma_{21}^- \rangle - E_2 \langle \sigma_{10}^\dagger \rangle - \frac{\gamma_{01}}{2} \langle \sigma_{10}^+ \rangle, \quad (\text{B2})$$

$$\frac{d\langle \sigma_{20}^\dagger \rangle}{dt} = -J\langle a^\dagger b \rangle \langle \sigma_{10}^+ \rangle + E_1 \langle \sigma_{20}^\dagger \rangle + E_2 \langle \sigma_{21}^+ \rangle - \frac{\gamma_{21}}{2} \langle \sigma_{20}^+ \rangle, \quad (\text{B3})$$

$$\begin{aligned}
\frac{d\langle \sigma_1 \rangle}{dt} & = J\langle a^\dagger b \rangle \langle \sigma_{21}^- \rangle - E_2 (\langle \sigma_{10}^+ \rangle - \langle \sigma_{10}^- \rangle) \\
& + \gamma_{21} \langle \sigma_2 \rangle - \gamma_{10} \langle \sigma_1 \rangle, \quad (\text{B4})
\end{aligned}$$

$$\frac{d\langle \sigma_2 \rangle}{dt} = -2J\langle a^\dagger b \rangle \langle \sigma_{21}^- \rangle - E_1 (\langle \sigma_{20}^+ \rangle + \langle \sigma_{20}^- \rangle) - \gamma_{21} \langle \sigma_2 \rangle, \quad (\text{B5})$$

$$\frac{d\langle \sigma_0 \rangle}{dt} = -\frac{d\langle \sigma_2 \rangle}{dt} - \frac{d\langle \sigma_1 \rangle}{dt}, \quad (\text{B6})$$

where we have considered the factorization of the form  $\langle a^\dagger b \sigma_{21}^- \rangle = \langle a^\dagger b \rangle \langle \sigma_{21}^- \rangle$ . Solving this set of equations and considering  $\{E_1, E_2, \gamma_{10}\} \gg \{J, \kappa_a, \kappa_b\}$  and  $\gamma_{21} = 0$  we get an expression for the atomic moment  $\langle \sigma_{21}^+ \rangle$  given by

$$\langle \sigma_{21}^+ \rangle = \frac{2E_1 E_2}{\gamma_{01}^2 + 4(E_1^2 + E_2^2)}. \quad (\text{B7})$$

From Eq. (B7), we can now easily derive the moments for the bosonic operators, necessary to calculate the relevant quadrature fluctuations:

$$\langle a^2 \rangle = -\frac{4J^2 \langle \sigma_{21}^+ \rangle^2 \kappa_b M_{sq}}{(\kappa_a + \kappa_b)(4J^2 \langle \sigma_{21}^+ \rangle^2 + \kappa_a \kappa_b)}, \quad (\text{B8})$$

$$\langle b^2 \rangle = M_{sq} \left( \frac{4J^2 \langle \sigma_{21}^+ \rangle^2 \kappa_a N_{sq}}{(\kappa_a + \kappa_b)(4J^2 \langle \sigma_{21}^+ \rangle^2 + \kappa_a \kappa_b)} - 1 \right), \quad (\text{B9})$$

$$\langle a^\dagger a \rangle = \frac{4J^2 \langle \sigma_{21}^+ \rangle^2 \kappa_b N_{sq}}{(\kappa_a + \kappa_b)(4J^2 \langle \sigma_{21}^+ \rangle^2 + \kappa_a \kappa_b)}, \quad (\text{B10})$$

$$\langle b^\dagger b \rangle = \frac{N_{sq} \kappa_b (4J^2 \langle \sigma_{21}^+ \rangle^2 + \kappa_a [\kappa_a + \kappa_b])}{(\kappa_a + \kappa_b)(4J^2 \langle \sigma_{21}^+ \rangle^2 + \kappa_a \kappa_b)}. \quad (\text{B11})$$

These last expressions allow us to directly calculate the Eqs. (14) and (15).

- 
- [1] M. Aspelmeyer, T. J. Kippenberg, and F. Marquardt, Cavity optomechanics, *Rev. Mod. Phys.* **86**, 1391 (2014).
- [2] C. Sánchez Muñoz, A. Lara, J. Puebla, and F. Nori, Hybrid Systems for the Generation of Nonclassical Mechanical States via Quadratic Interactions, *Phys. Rev. Lett.* **121**, 123604 (2018).
- [3] M. Mirhosseini, A. Sipahigil, M. Kalaei, and O. Painter, Superconducting qubit to optical photon transduction, *Nature (London)* **588**, 599 (2020).
- [4] D. Hunger, S. Camerer, T. W. Hänsch, D. König, J. P. Kotthaus, J. Reichel, and P. Treutlein, Resonant Coupling of a Bose-Einstein Condensate to a Micromechanical Oscillator, *Phys. Rev. Lett.* **104**, 143002 (2010).
- [5] G. A. Steele, A. K. Hüttel, B. Witkamp, M. Poot, H. B. Meerwaldt, L. P. Kouwenhoven, and H. S. J. van der Zant, Strong coupling between single-electron tunneling and nanomechanical motion, *Science* **325**, 1103 (2009).
- [6] S. G. Carter, A. S. Bracker, G. W. Bryant, M. Kim, C. S. Kim, M. K. Zalalutdinov, M. K. Yakes, C. Czarnocki, J. Casara, M. Scheibner, and D. Gammon, Spin-Mechanical Coupling of an InAs Quantum Dot Embedded in a Mechanical Resonator, *Phys. Rev. Lett.* **121**, 246801 (2018).
- [7] E. R. MacQuarrie, T. A. Gosavi, S. A. Bhave, and G. D. Fuchs, Continuous dynamical decoupling of a single diamond nitrogen-vacancy center spin with a mechanical resonator, *Phys. Rev. B* **92**, 224419 (2015).
- [8] M. Abdi, M.-J. Hwang, M. Aghtar, and M. B. Plenio, Spin-Mechanical Scheme with Color Centers in Hexagonal Boron Nitride Membranes, *Phys. Rev. Lett.* **119**, 233602 (2017).
- [9] I. Marinković, A. Wallucks, R. Riedinger, S. Hong, M. Aspelmeyer, and S. Gröblacher, Optomechanical Bell Test, *Phys. Rev. Lett.* **121**, 220404 (2018).
- [10] N. Aggarwal, T. J. Cullen, J. Cripe, G. D. Cole, R. Lanza, A. Libson, D. Follman, P. Heu, T. Corbitt, and N. Mavalvala, Room-temperature optomechanical squeezing, *Nat. Phys.* **16**, 784 (2020).
- [11] T. Li, S. Kheifets, and M. G. Raizen, Millikelvin cooling of an optically trapped microsphere in vacuum, *Nat. Phys.* **7**, 527 (2011).
- [12] J. Guo, R. Norte, and S. Gröblacher, Feedback Cooling of a Room Temperature Mechanical Oscillator Close to its Motional Ground State, *Phys. Rev. Lett.* **123**, 223602 (2019).

- [13] D. D. B. Rao, S. A. Momenzadeh, and J. Wrachtrup, Heralded Control of Mechanical Motion by Single Spins, *Phys. Rev. Lett.* **117**, 077203 (2016).
- [14] Y. Nakamura, Y. A. Pashkin, and J. S. Tsai, Coherent control of macroscopic quantum states in a single-cooper-pair box, *Nature (London)* **398**, 786 (1999).
- [15] J.-Q. Liao and L. Tian, Macroscopic Quantum Superposition in Cavity Optomechanics, *Phys. Rev. Lett.* **116**, 163602 (2016).
- [16] V. Montenegro, R. Coto, V. Eremeev, and M. Orszag, Macroscopic nonclassical-state preparation via postselection, *Phys. Rev. A* **96**, 053851 (2017).
- [17] R. Y. Teh, S. Kiesewetter, P. D. Drummond, and M. D. Reid, Creation, storage, and retrieval of an optomechanical cat state, *Phys. Rev. A* **98**, 063814 (2018).
- [18] M. Scala, M. S. Kim, G. W. Morley, P. F. Barker, and S. Bose, Matter-Wave Interferometry of a Levitated Thermal Nano-Oscillator Induced and Probed by a Spin, *Phys. Rev. Lett.* **111**, 180403 (2013).
- [19] K. Stannigel, P. Rabl, A. S. Sørensen, P. Zoller, and M. D. Lukin, Optomechanical Transducers for Long-Distance Quantum Communication, *Phys. Rev. Lett.* **105**, 220501 (2010).
- [20] R. Riedinger, S. Hong, R. A. Norte, J. A. Slater, J. Shang, A. G. Krause, V. Anant, M. Aspelmeyer, and S. Gröblacher, Non-classical correlations between single photons and phonons from a mechanical oscillator, *Nature (London)* **530**, 313 (2016).
- [21] A. P. Reed, K. H. Mayer, J. D. Teufel, L. D. Burkhardt, W. Pfaff, M. Reagor, L. Sletten, X. Ma, R. J. Schoelkopf, E. Knill, and K. W. Lehnert, Faithful conversion of propagating quantum information to mechanical motion, *Nat. Phys.* **13**, 1163 (2017).
- [22] L. Robledo, L. Childress, H. Bernien, B. Hensen, P. F. A. Alkemade, and R. Hanson, High-fidelity projective read-out of a solid-state spin quantum register, *Nature (London)* **477**, 574 (2011).
- [23] V. Giovannetti, S. Lloyd, and L. Maccone, Quantum Metrology, *Phys. Rev. Lett.* **96**, 010401 (2006).
- [24] B. E. Anderson, P. Gupta, B. L. Schmittberger, T. Horrom, C. Hermann-Avigliano, K. M. Jones, and P. D. Lett, Phase sensing beyond the standard quantum limit with a variation on the  $su(1,1)$  interferometer, *Optica* **4**, 752 (2017).
- [25] N. S. Kampel, R. W. Peterson, R. Fischer, P.-L. Yu, K. Cicak, R. W. Simmonds, K. W. Lehnert, and C. A. Regal, Improving Broadband Displacement Detection with Quantum Correlations, *Phys. Rev. X* **7**, 021008 (2017).
- [26] D. Mason, J. Chen, M. Rossi, Y. Tsaturyan, and A. Schliesser, Continuous force and displacement measurement below the standard quantum limit, *Nat. Phys.* **15**, 745 (2019).
- [27] J. Aasi, Enhanced sensitivity of the ligo gravitational wave detector by using squeezed states of light, *Nat. Photonics* **7**, 613 (2013).
- [28] H. Grote, K. Danzmann, K. L. Dooley, R. Schnabel, J. Slutsky, and H. Vahlbruch, First Long-Term Application of Squeezed States of Light in a Gravitational-Wave Observatory, *Phys. Rev. Lett.* **110**, 181101 (2013).
- [29] P. E. Allain, L. Schwab, C. Mismar, M. Gely, E. Mairiaux, M. Hermouet, B. Walter, G. Leo, S. Hentz, M. Faucher, G. Jourdan, B. Legrand, and I. Favero, Optomechanical resonating probe for very high frequency sensing of atomic forces, *Nanoscale* **12**, 2939 (2020).
- [30] F. He, J. Liu, and K.-D. Zhu, Optomechanical atomic force microscope, *Nanotechnology* **32**, 085505 (2021).
- [31] X.-Y. Lü, J.-Q. Liao, L. Tian, and F. Nori, Steady-state mechanical squeezing in an optomechanical system via duffing nonlinearity, *Phys. Rev. A* **91**, 013834 (2015).
- [32] S. Liu, W.-X. Yang, Z. Zhu, T. Shui, and L. Li, Quadrature squeezing of a higher-order sideband spectrum in cavity optomechanics, *Opt. Lett.* **43**, 9 (2018).
- [33] J.-S. Zhang and A.-X. Chen, Large mechanical squeezing beyond 3dB of hybrid atom-optomechanical systems in a highly unresolved sideband regime, *Opt. Express* **28**, 12827 (2020).
- [34] D.-Y. Wang, C.-H. Bai, S. Liu, S. Zhang, and H.-F. Wang, Dissipative bosonic squeezing via frequency modulation and its application in optomechanics, *Opt. Express* **28**, 28942 (2020).
- [35] D. W. C. Brooks, T. Botter, S. Schreppler, T. P. Purdy, N. Brahms, and D. M. Stamper-Kurn, Non-classical light generated by quantum-noise-driven cavity optomechanics, *Nature (London)* **488**, 476 (2012).
- [36] A. H. Safavi-Naeini, S. Gröblacher, J. T. Hill, J. Chan, M. Aspelmeyer, and O. Painter, Squeezed light from a silicon micromechanical resonator, *Nature (London)* **500**, 185 (2013).
- [37] T. P. Purdy, P.-L. Yu, R. W. Peterson, N. S. Kampel, and C. A. Regal, Strong Optomechanical Squeezing of Light, *Phys. Rev. X* **3**, 031012 (2013).
- [38] J.-M. Pirkkalainen, E. Damskägg, M. Brandt, F. Massel, and M. A. Sillanpää, Squeezing of Quantum Noise of Motion in a Micromechanical Resonator, *Phys. Rev. Lett.* **115**, 243601 (2015).
- [39] E. E. Wollman, C. U. Lei, A. J. Weinstein, J. Suh, A. Kronwald, F. Marquardt, A. A. Clerk, and K. C. Schwab, Quantum squeezing of motion in a mechanical resonator, *Science* **349**, 952 (2015).
- [40] C. F. Ockeloen-Korppi, E. Damskägg, G. S. Paraoanu, F. Massel, and M. A. Sillanpää, Revealing Hidden Quantum Correlations in an Electromechanical Measurement, *Phys. Rev. Lett.* **121**, 243601 (2018).
- [41] J. Czartowski, R. Müller, K. Życzkowski, and D. Braun, Perfect quantum-state synchronization, *Phys. Rev. A* **104**, 012410 (2021).
- [42] E. Massoni and M. Orszag, Squeezing transfer from vibrations to a cavity field in an ion-trap laser, *Opt. Commun.* **190**, 239 (2001).
- [43] R. Rangel, L. Carvalho, and N. Zagury, Squeezing generation and revivals in a cavity-ion system in contact with a reservoir, *J. Phys. B: At. Mol. Opt. Phys.* **38**, 729 (2005).
- [44] L. Liu, B.-P. Hou, X.-H. Zhao, and B. Tang, Squeezing transfer of light in a two-mode optomechanical system, *Opt. Express* **27**, 8361 (2019).
- [45] M. Wallquist, K. Hammerer, P. Zoller, C. Genes, M. Ludwig, F. Marquardt, P. Treutlein, J. Ye, and H. J. Kimble, Single-atom cavity QED and optomechanics, *Phys. Rev. A* **81**, 023816 (2010).
- [46] F. Momeni and M. H. Naderi, Atomic quadrature squeezing and quantum state transfer in a hybrid atom-optomechanical cavity with two Duffing mechanical oscillators, *J. Opt. Soc. Am. B* **36**, 775 (2019).
- [47] C.-H. Bai, D.-Y. Wang, S. Zhang, S. Liu, and H.-F. Wang, Engineering of strong mechanical squeezing via the joint effect between duffing nonlinearity and parametric pump driving, *Photonics Res.* **7**, 1229 (2019).

- [48] J. R. Johansson, P. D. Nation, and F. Nori, *Comput. Phys. Commun.* **184**, 1234 (2013).
- [49] M. A. Nielsen and I. L. Chuang, *Quantum Computation and Quantum Information*, 2nd ed. (Cambridge University Press, Cambridge, 2010)
- [50] T. Carmon, H. Rokhsari, L. Yang, T. J. Kippenberg, and K. J. Vahala, Temporal Behavior of Radiation-Pressure-Induced Vibrations of an Optical Microcavity Phonon Mode, *Phys. Rev. Lett.* **94**, 223902 (2005).
- [51] T. J. Kippenberg, H. Rokhsari, T. Carmon, A. Scherer, and K. J. Vahala, Analysis of Radiation-Pressure Induced Mechanical Oscillation of an Optical Microcavity, *Phys. Rev. Lett.* **95**, 033901 (2005).